Phobos Magnetic Field

Note 00-001

Patrick Decowski, decowski@mit.edu
Leslie Rosenberg, ljr@mitlns.mit.edu

February 15, 2000

`$Id: mag_field.tex,v 1.6 2000/02/15 23:42:01 decowski Exp $`

1 Purpose and Scope

The magnetic field of the Phobos magnet was measured in February and March of 1999. This document describes the measurements and the subsequent processing of the raw data to turn it into a useful map for Phobos. It is a follow-up on the 'Phobos Magnetic Field Mapping' [Ros99] which describes the mapping plan. We will first describe the results from the detailed survey of the mapper, then some general properties of the magnetic field. Next, we will discuss some corrections to the fields and the interpolation. Finally, a comparison will be made between the measured field and the simulated TOSCA field.

2 Magnetic field measurement device

We used the AGS magnetic field mapper [Hoe98] to do the mapping. A sketch of the apparatus is presented in figure 1. It consists of five parts: (1) the moving mapping stage; (2) three Hall probes with gaussmeters, one for each magnetic field component; (3) a roll and tilt-sensor to establish the vertical direction; (4) the sensor cart containing the Hall probes and the tilt sensor; (5) the data acquisition computer.

The mapping stage can move along three Cartesian axes (see figure 1). There is 72 inches (183cm) and 48 inches (122cm) of travel in the horizontal direction, and 36 inches (91cm) in the vertical direction. Only travel in the

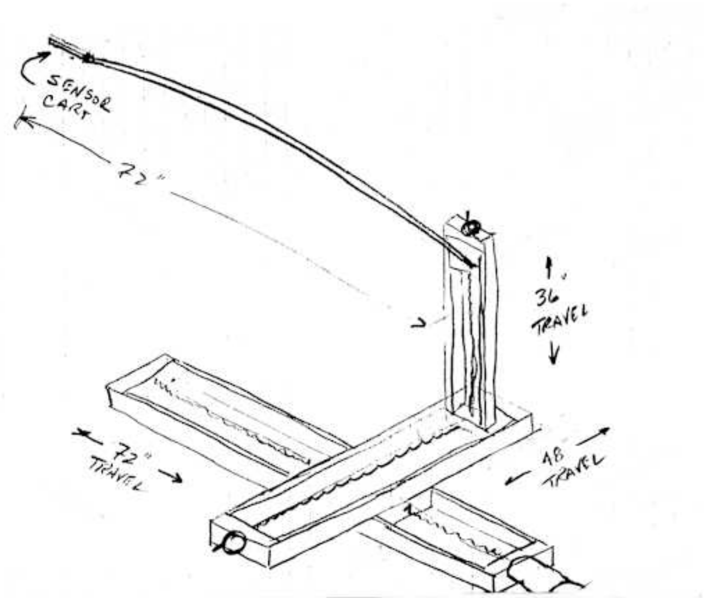

Figure 1: Sketch of the AGS mapping station.

72 inch direction is automated. The other two directions have to be adjusted manually.

Since the reach of the mapper is limited, the mapper was used in two positions: an 'inner arm' and an 'outer arm' position. The 'inner arm' position refers to the spectrometer arm in the negative X direction and the 'outer arm' is the positive X direction arm. The two regions had an overlap area of about $12cm$.

The measurements were taken at three different current settings: $3600A$ (full field), $3500A$ and $2700A$. We monitored the shunt voltage of the magnet power supply, which is directly proportional to the current. The shunt voltage was found to be stable to a few parts in 10000.

One 72inch trajectory took about 30min to complete taking measurements every inch. Due to time limitations, it was decided to concentrate on getting a detailed field at full current and limit the number of trajectories for the two other current settings. Table 1 shows the trajectory spacing.

Current (A)	Spacing in X	Spacing in Y	Spacing in Z
3600	21x2inch	5x2.75cm	72x1inch
3500	11x4inch	3x3cm	72x1inch
2700	11x4inch	3x3cm	72x1inch

Table 1: Spacing between the traces

3 Survey

The AGS survey group spent 10 days taking detailed survey measurements of the mapper setup, measuring several hundred points. The surveying had two purposes: (1) to establishing the mapping between the magnet coordinate system (readings on the mapper) and the survey coordinate system and (2) to position the mapper inside the RHIC coordinate system. The RHIC coordinate system is the coordinate system to which all Phobos components will be referenced.

The survey allowed us to translate mapper coordinates into RHIC coordinates. We found this translation to be very reproducible. In the following two sections we describe the main corrections to mapper coordinates.

3.1 'Bowing' of the mapper

Figure 2 shows the 'bowing' due to the weight of the probing structure of the horizontal cross-bar of the mapper, as the vertical cross-bar is moved. The vertical drop is 1.5mm between the middle position (X=10" in mapper coordinates) and the outer positions. Additionally, a counterweight was used for the outer three mapping points on either side, to prevent mechanical binding of the mapper when the weight is not distributed uniformly.

3.2 Track height non-uniformity

Figure 3 shows an additional deformation: the center track was not uniform in height. This was first measured by us using the surveying information and later in more detail re-measured by the AGS Magnetic Measurements Group. For this we also made a global correction.

3.3 Final Survey corrections

With the detailed (non-linear) mapping between the coordinate system of the magnet and the survey in hand, the magnet still needed positioning in

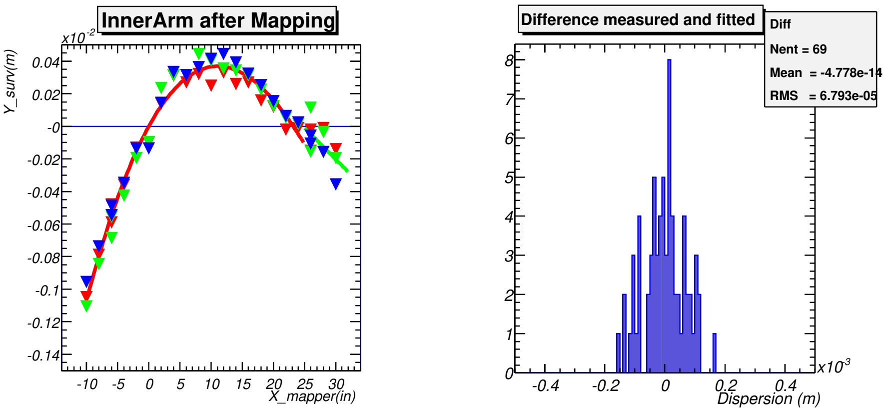

Figure 2: Global fit of the 'bowing' of the mapper, at the 'Inner Arm' position. The left hand plot shows the 'bowing' of the mapping station as a function of the horizontal position of the mapper. To improve statistics all survey points were lumped together after taking out a common offset, then a global parametrization of the 'bowing' was performed. Right hand plot shows the comparison of the calculated Y position using the parametrization to the survey results. The dispersion is $\approx 70\mu m$ which is comparable to the survey error.

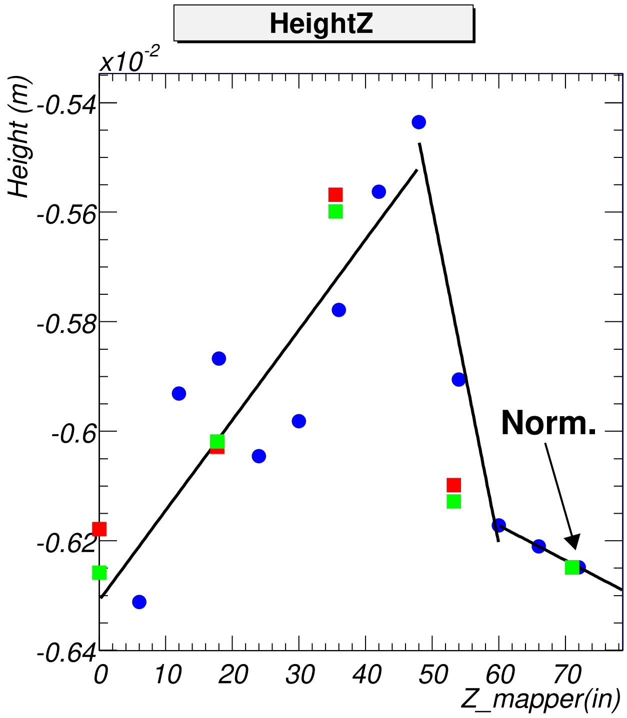

Figure 3: Non-uniformity of the flatness of the track of the mapper. The round points show (post mapping) detailed height measurements of the track flatness. The square points are from the magnet survey data. An arbitrary overall constant was taken out of the two datasets by normalizing to the last point.

the RHIC coordinate system. This was done with another set of survey corrections. First, the magnet coordinates were transformed into 'survey coordinates' using the parametrizations described in the previous two sections. Then, using all available survey points for a given arm, a 3x3 matrix and a vector translation was fitted. The components of the 3x3 matrix describe the rotations and any remaining skews of the system. Figure 4 shows the deviation of the calculated RHIC positions of the mapper using all the above corrections from the positions measured by the AGS surveyors. The observed dispersion is between $\approx 80\mu m$ in the Y direction and a maximum of $\approx 190\mu m$ in the X direction. Similar values were obtained for both mapper positions.

In the 'Mapping Plan' [Ros99], we estimated that the mapper positioning error would be $100\mu m$ in the vertical direction and $125\mu m$ in the horizontal directions.

4 General Properties of the Magnet

4.1 Excitation Curve

The excitation curve of the magnet was measured with a handheld Gaussmeter. The meter was positioned in such a way as to measure the B_y component of the field at the highest field point. The excitation curve is presented in figure 5. The iron saturation at about $2500A$ becomes evident.

4.2 Magnetic Safety: 5 and 10 Gauss lines

The 5 and 10 Gauss magnetic field lines had to be established for magnetic safety considerations. Figure 6 shows a contour plot of these two lines.

4.3 Zero current map

The residual, zero current, field was determined to be insignificant, even after having had the magnet on for several weeks (less than 3 Gauss at the pole surface).

5 Roll and Pitch

The mapping sensor truck had a roll and pitch sensor to measure the tilt of the axis of the three Hall probes. This ensures that the three magnetic field components can be clearly separated, without mixing between them.

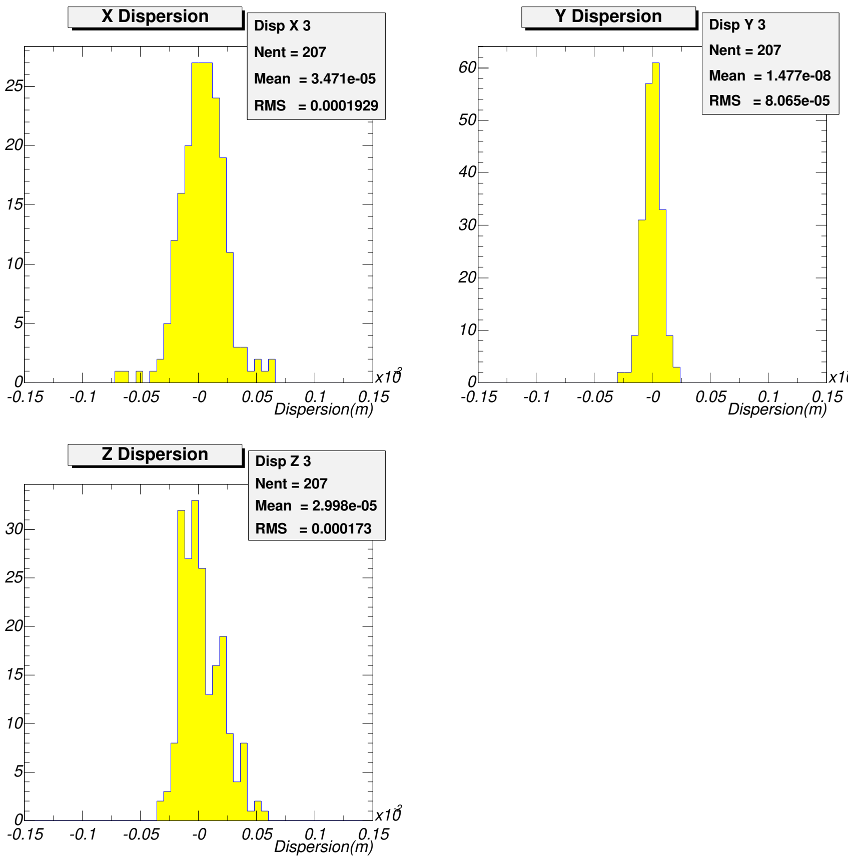

Figure 4: Dispersion in the three directions between the corrected mapper coordinates and the directly measured survey coordinates.

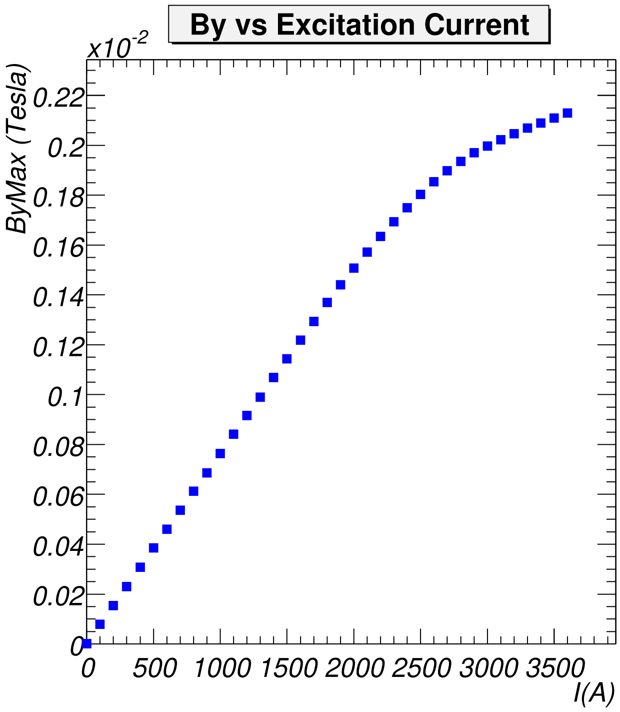

Figure 5: Excitation curve of the magnet. The magnetic field was measured at the highest By component.

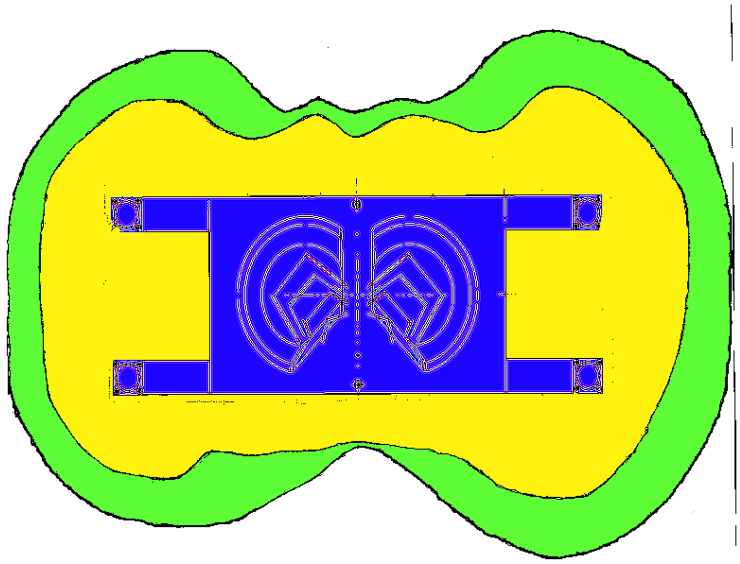

Figure 6: 10 Gauss (inner) and 5 Gauss (outer) contour lines of the magnetic field in a top view. Also visible is an outline of the magnet. To indicate the scale: the total width of the magnet is 140cm

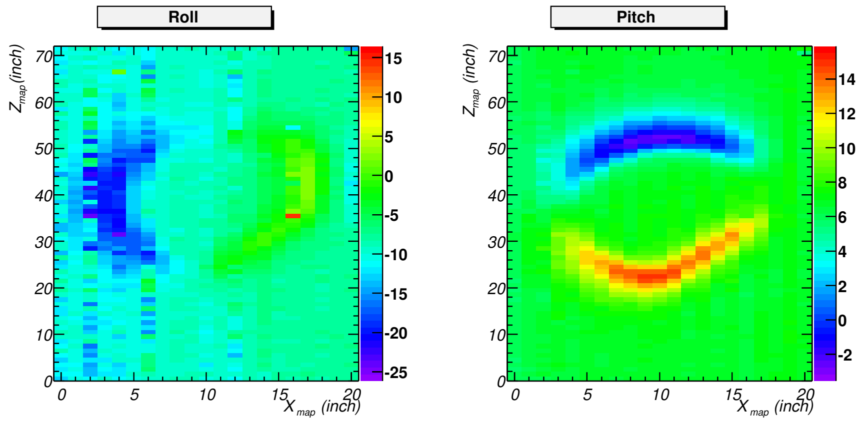

Figure 7: The Hall probes on the mapper were not entirely parallel to the RHIC coordinate system. A roll and a pitch sensor was used to correct any field component mixing. This plot shows the sensor angle (in mrad). The roll and pitch were disturbed in the highest field gradients.

Spectrometer Side	Roll (mrad)	Pitch (mrad)
Inner Arm	-5.40	-0.14
Outer Arm	-8.95	6.75

Table 2: Roll and pitch angles at the two mapping positions

It was found that the angle sensors were disturbed by the high magnetic field gradient during the field measurements. This rendered the angle measurements in the high field gradient region difficult to interpret, other than that the angles did not change significantly over the entire region. Therefore we average the roll and pitch values over the first few inches of travel (where the field is still small) and use these averages to correct the field components. Table 2 shows the values for the roll and pitch angles for both mapping positions.

6 Overlap region

As already mentioned in section 2, the two mapper positions had an area of overlap of $\approx 12cm$. Figure 8 shows a combined view of the three magnetic field components for a slice in X through the overlap region. It is clearly visible that the two regions join smoothly.

7 Interpolation

The measured field points are on a non-rectangular grid due to the mechanical deformations of the mapper. We interpolate the non-rectangular grid to produce a field map on a uniformly spaced, $1 \times 1 \times 1cm$ grid. This is the same grid as was used for the TOSCA simulations. The software then only has to linearly interpolate between two adjacent grid points in this new grid.

To test the interpolation and get an estimate on the interpolation error, the following test was performed. Take the measured map and interpolate between every 2nd point in the Z direction. The obtained field value is then compared to the measured value at the same position. The top left plot of figure 9 shows the interpolated values in Gauss, the right plot shows the distribution of the difference between the interpolated and the actually measured value (also in Gauss) and the lower plot shows the fractional error. The interpolation usually contributes less than 2 permille in the field error, only in the regions where the field rapidly changes (such as near the coils) is the error ≈ 6 permille. A 4th order polynomial was found to give good results during this study. In our case, the error will be actually smaller, because the interpolation does not have to be over a distance of 2inches in Z, but only 1inch.

8 Comparison with Simulated field

With the field map ready, a comparison was made between the TOSCA simulated field and the final field map. Figure 10 shows the comparison for the B_y component, with the sensor planes superimposed on the plot. The plot shows that the field is 10% smaller than expected in the low field region and 10% higher in the high field region. This can probably be attributed to the higher quality iron that was used for the pole than originally specified. The B_x and B_z components also agree quite well. Only where the field is small (≈ 10 Gauss) relative deviations can be large.

9 Conclusion

The final field map of the Phobos magnet, including all the necessary corrections is ready. The map grid size of $1 \times 1 \times 1cm$ is exactly the same as

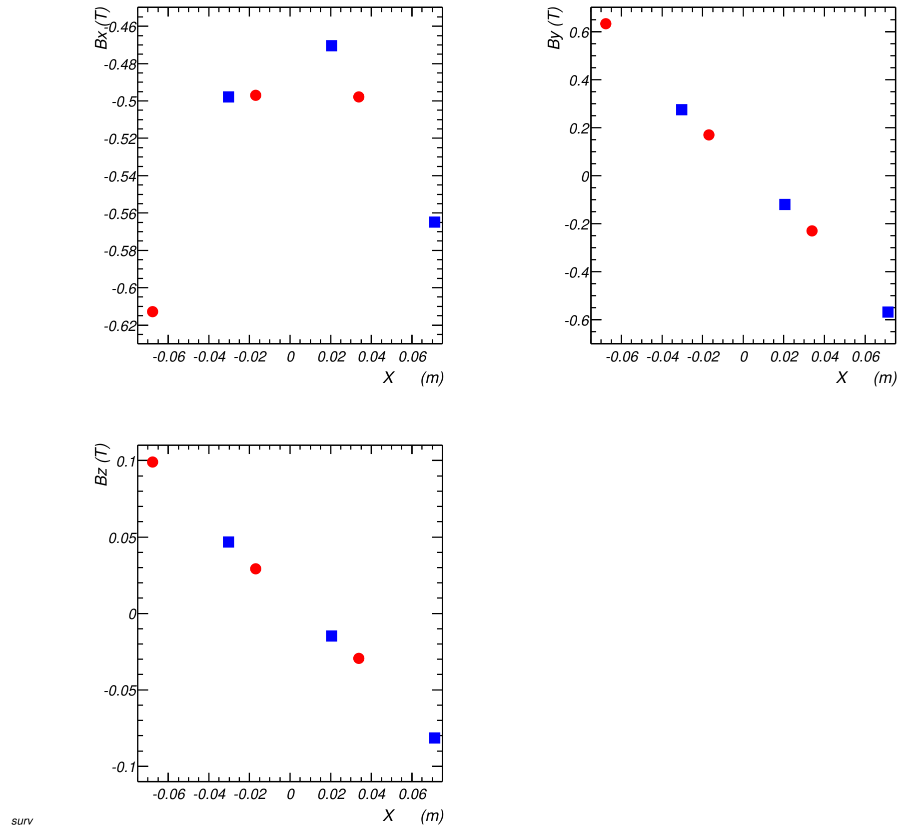

Figure 8: Plot of the three magnetic field components in the overlap region. The plots show a slice in X for $Y = 0cm$ and $Z = 0.54cm$. The square points belong to measurements taken with the mapper positioned in the 'Outer Arm' position, the round points show the measurements taken in the 'Inner Arm' position.

that of the simulated map. This should make the integration of the new field map into existing software easy.

References

[Ros99] Rosenberg, L.J. *Phobos Magnetic Field Mapping*, Phobos Note 99-???, January 1999.

[Hoe98] Hoey, E., *Field Mapper Information*, Magnetic Measurements Group at the AGS, September 1998.

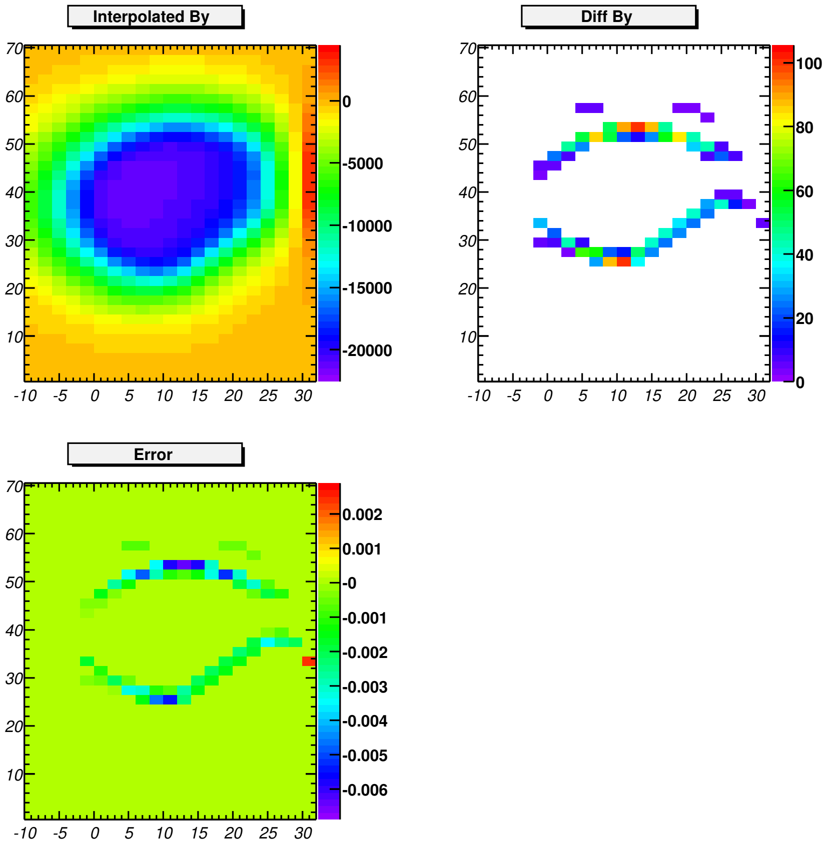

Figure 9: Interpolation test. An interpolation was performed between every 2nd point in the Z direction. The interpolated value was then compared to the measured value. The lower left plot shows that near the coils a maximum interpolation error of 6 permille is obtained.

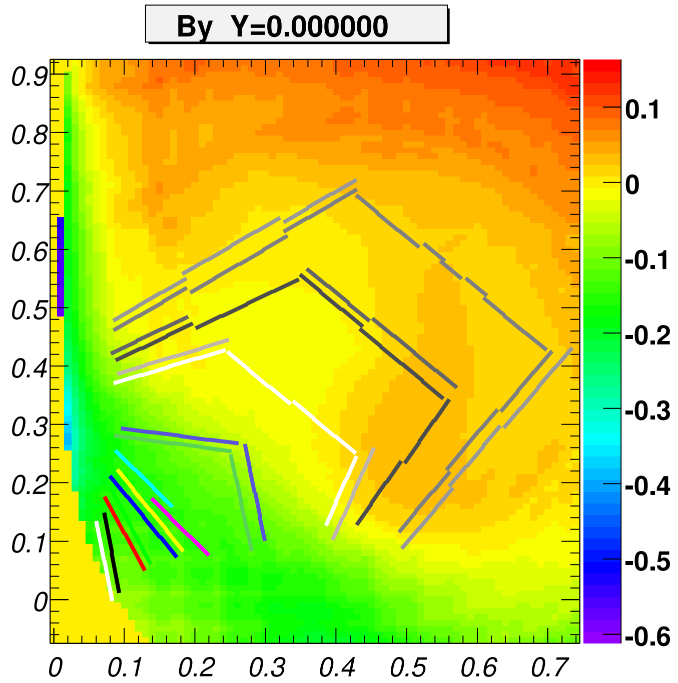

Figure 10: Compare field on non rectangular grid with the simulated TOSCA field. The fractional difference, $\frac{B_y^{meas} - B_y^{sim}}{B_y^{meas}}$ is plotted. One can see that the field is 10% smaller than expected in the low field region and 10% higher in the high field region. The sensor planes are also shown.